Nuclear Magnetism in Solid Methane*

R. Fraser Code

Department of Physics and Erindale College
University of Toronto
Toronto Canada
M5S 1A7

I. Introduction

For more than 30 years, the observation of nuclear magnetic interactions in solid methane has given valuable information on the reorientational dynamics of its molecules. Recently, measurements of some basic properties of nuclear absorption lineshapes, such as the integrated intensity and the second moment, have revealed the rates at which the populations of various molecular orientational states approach thermal equilibrium.

The study of solid methane has attracted widespread attention from physicists and chemists for good reason. As is the case with solid hydrogen, solid methane and its deuterated isotopes are relatively simple materials. They offer the theorist the challenge of predicting the structure and properties of the solid phases from first principles because detailed information is available about the molecular wavefunctions and binary intermolecular potentials.

The properties of solid methane that are important for NMR can be briefly summarized as follows. At zero external pressure it has two stable phases. Between the triple point at 90.6861 K (1) and ~20.4 K it exists in an orientationally disordered structure (phase I) with the center of mass of the molecules arranged on a FCC lattice. At temperatures below ~20.4 K the weak anisotropic forces between molecules establish a new structure (phase II) having partial "antiferrorotational" order. The transition between phases I and II displays a small thermal hysteresis (2). In phase II, 75% of the molecules are orientationally ordered on six out of eight interpenetrating sublattices. This structure was predicted classically by James and Keenan (3). The remaining 25% of the molecules on the other two sublattices are rotationally disordered.

The mass of methane molecules is sufficiently large that translational motions in the solid are essentially classical. This is not true for the rotational degrees of freedom however.

---

*Presented at the 7th Waterloo NMR Summer School, June 9, 1981

The moments of inertia of methane are quite small, and give rise to observable "rotational quantum effects."

Weak intramolecular hyperfine interactions provide the only means of coupling the nuclear magnetic moments to the reorientational motions of the molecule (4). It is often convenient to neglect these interactions, and consider that the nuclear wavefunction of the four protons in CH_4 evolves independently in time from the rest of the molecular wavefunction. This approximation leads to the factorization of the nuclear and rotational parts of the wavefunction, and to the treatment of solid methane as an "alloy" of three distinct nuclear spin symmetry species having a fixed ratio of A, T and E populations (5). In this approximation, conversion between the three spin species is strictly forbidden.

However, NMR experiments are able to observe solid methane for such long times at liquid helium temperature that the effects of intramolecular hyperfine coupling cannot be neglected. In fact, the population ratios of A, T and E states in the solid are known to change slowly with time (6). The reason why such changes occur has a relatively simple explanation. The energy splittings between the low lying orientational or "tunneling" states of the molecules in phase II are comparable to thermal energies of several degrees Kelvin. But these tunneling levels are not eigenstates with pure A, T or E nuclear spin symmetry because magnetic dipole-dipole interactions between the protons within a single molecule introduce a coupling between states of different total nuclear spin. Hence at low temperatures a pathway exists for a slow conversion between all tunneling states by the exchange of angular momentum and orientational energy with the lattice (7). The unusual feature of this "spin-symmetry conversion" in phase II of solid methane is that its rate is much faster for the 25% of molecules which are on rotationally disordered sublattices compared to the remaining 75% on orientationally ordered sublattices (8). In the following sections we will review our cw NMR susceptibility measurements which determined the short and long term equilibrium spin-symmetry populations in solid methane. Some previously unpublished data are presented.

II. The Magnetic Susceptibility of the Protons

The temperature dependence of the static proton magnetic susceptibility in solid methane is governed by Curie's law:

$$\chi_o^p = \frac{N\gamma_p^2\hbar^2 \langle I(I+1)\rangle_p}{3kT} \qquad (1)$$

where N is the number density of molecules, γ is the gyromagnetic ratio of the proton, $\hbar$ is Planck's constant, $\langle I(I+1)\rangle_p$ is the mean square proton k is Boltzman's constant, and T is the temperature in Kelvin. The deviation of this susceptibility from a strict (1/T) temperature dependence (or equivalently, variations in the value of $\langle I(I+1)\rangle_p$) is a direct probe of changes in the proton spin-symmetry populations. In ^{13}C labelled solid methane, variations in the value of $\langle I(I+1)\rangle_p$ can be independently monitored by the ratio of the magnetic susceptibility of the protons to the susceptibility of the ^{13}C nuclei:

$$\langle I(I+1)\rangle_p \equiv 6P_A + 2P_T = \qquad (2)$$

$$(3/4)\,\eta\,(\gamma_{^{13}C}/\gamma_p)^2\,(\chi_o^p/\chi_o^{^{13}C})$$

where P_A and P_T are the relative populations of the A and T symmetry species, η is the fraction of molecules labelled with ^{13}C, $\gamma_{^{13}C}$ is the gyromagnetic ratio of the ^{13}C nucleus, and $\chi_o^{^{13}C}$ is the static susceptibility of the ^{13}C nuclei. The use of ^{13}C nuclei as an internal spin thermometer for these measurements of $\langle I(I+1)\rangle_p$ makes the results insensitive to small thermal gradients across the sample. This method also produces accurate

comparisons of spin-isomer population ratios over a very wide temperature range. In addition, the ^{13}C label does not perturb the resulting values of $\langle I(I+1)\rangle_p$ for two reasons: (a) it increases the mass of the molecule by such a small amount that it does not significantly interfere with the lattice dynamics; and (b) the ^{13}C nucleus at the center of symmetry of the molecule is coupled to the proton spins within the same molecule by very weak magnetic interactions that do not significantly influence the spin species conversion rates.

The susceptibility ratio, equation 2, can be determined by various pulsed (6) and cw (8,9) NMR techniques. For precise observations of nuclear magnetic susceptibility ratios at conditions close to equilibrium, it is often most convenient to use a simple cw Q meter circuit (10) because of its rf stability and ease of calibration. All of the relative proton and ^{13}C susceptibilities in our experiments below were determined by double integrations of digitized derivative adsorption lineshapes, observed at a common fixed frequency (9,11,12). The relative susceptibilities were calibrated for all samples by observations at temperatures near 100 K, where the relative populations of A, T and E spin-symmetry states are in the classical ratio of 5 : 9 : 2.

In order to have results that are reproducible over long periods of time, the various methane samples studied were stored in sealed glass containers, such as shown in Figure 1. An oxygen-free sample of $^{13}CH_4$ was prepared by activating the Misch-metal getter (13) before the tube was filled. This sample was used for the determination of the intrinsic rate of proton spin-species conversion (9). Samples were also made of CH_4 containing trace O_2 impurities and $^{13}CH_4$ adsorbed in commercial grade Linde TM type 5A and 13X zeolites. A significant degree of conversion (i.e., comparable to that which occurs in solid CH_4 itself) was also

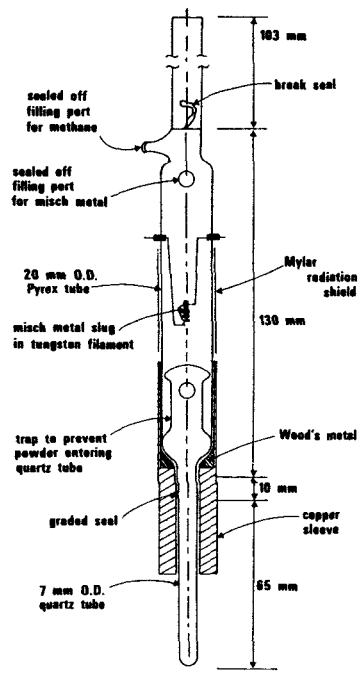

Figure 1. Sealed sample tube used for the determination of proton spin conversion rates in oxygen-free solid $^{13}CH_4$. The mylar radiation shield, the copper sleeve and the quartz tube at the bottom reduce thermal gradients across the solid methane in our helium gas-flow cryostat.

observed in $^{13}CH_4$ adsorbed in the synthetic type 5A and 13X zeolites at temperatures below 10 K (14). This can be interpreted as strong evidence that fairly large tunnel splittings persist when methane is adsorbed on surfaces.

III. Conversion and Second Moments in Solid $^{13}CH_4$

A thermal equilibrium between the populations of A, T, and E symmetry species is established fairly rapidly in solid methane samples containing small amounts of oxygen impurities. To

compare the results of the temperature dependence of $\langle I(I+1)\rangle_p$ with theory, it is necessary to know the energy levels of the tunneling eigenstates on both the 6 ordered and 2 rotationally disordered sublattices in phase II. These energy levels have been measured by inelastic neutron scattering experiments, and are known to vary with temperature (15,16), as shown in Figure 2.

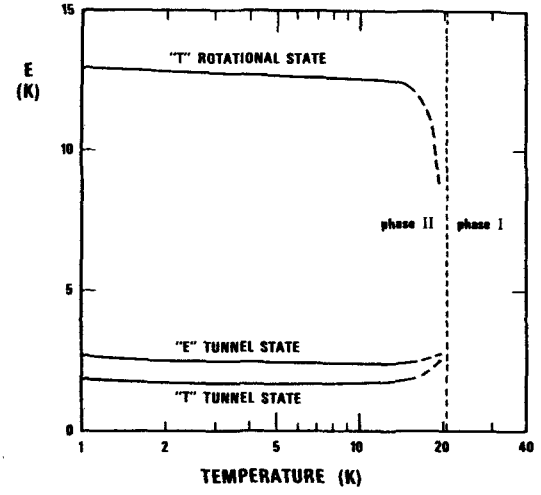

Figure 2. Energy levels of the excited orientational energy levels in phase II of solid methane above the respective ground state "A" energy levels for molecules on the two "disordered" sublattices (top line) and the six "ordered" sublattices (bottom two lines).

Using these energy levels, both "short-term" (conversion only on the two disordered sublattices) and "long-term" (conversion on all sublattices) equilibrium values of $\langle I(I+1)\rangle_p$ were calculated by simple Boltzman statistics. The results are compared with experimental values in Figure 3.

There is a satisfactory agreement between experiment and the theoretical curves for $\langle I(I+1)\rangle_p$ shown in Figure 3. In principle, measurements of $\langle I(I+1)\rangle_p$ from the susceptibility ratio given in equation 2 should be as accurate as the long term stability of the spectrometer, which was approximately $\pm 0.5\%$ for the reported experiment. In principle this is sufficiently precise to test the accuracy of the energy levels of the tunneling states observed by neutron scattering. However, in practice, the precision of the susceptibility ratio is limited to a few per cent by restrictions on the length of time available to observe the integrated absorption lineshape intensity of the weaker ^{13}C resonance.

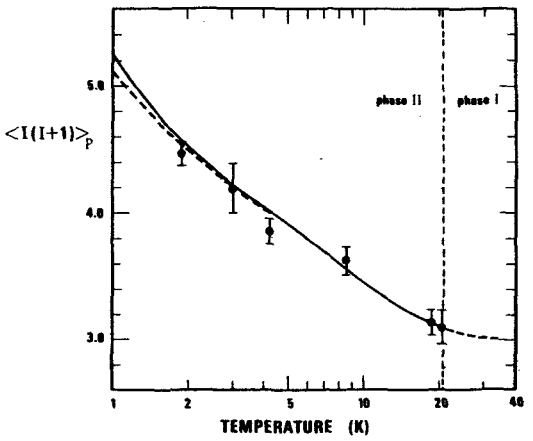

Figure 3. A comparison of calculated and observed equilibrium values of $\langle I(I+1)\rangle_p$ in phase II of solid CH_4. The dashed line below the solid curve was calculated by assuming the energy levels to be independent of temperature below 4.2 Kelvin. Equilibrium populations were obtained experimentally by doping the solid methane with ~500 ppm O_2.

There are also noticeable changes in the width of the absorption lineshapes of both the proton and the ^{13}C resonances as a result of conversion (17). The intramolecular contributions to the proton second moment in solid methane are "motionally" averaged to zero even at 2 K. Changes in the proton second moment in solid $^{13}CH_4$ are therefore dominated by intermolecular spin-spin

interactions, and are strongly correlated with changes in the value of $\langle I(I+1)\rangle_p$. Changes in $\langle I(I+1)\rangle_p$ are also correlated with the experimental values of the second moment of the ^{13}C resonance because its linewidth is largely determined by intermolecular proton-carbon spin-spin interactions (17).

The proton second moment in phase II of solid methane is not straight-forward to calculate because of its eight-sublattice antiferrorotational FCC structure. However, Nijman and Trappeniers (18,19) have shown how the Van Vleck theory of second moments should be applied to this problem. They begin with a general expression for the second moment in terms of the density matrix ρ:

$$M_z = -(1/\hbar^2)\,\frac{tr\{\rho[H'_{dd},\mu_x]^2\}}{tr\{\rho\mu_x^2\}} \qquad (3)$$

where H'_{dd} is the secular part of the dipole-dipole interaction Hamiltonian, and μ_x is the x component of the total magnetic moment.

This equation is used to calculate the intermolecular second moment of a pair of methane molecules separated by a distance $\vec{r}_{\alpha\beta}$. The density matrix ρ for the combined system is the product of the density matrices of the individual systems:

$$\rho = \rho(\alpha) \times \rho(\beta) \qquad (4)$$

Hence equation 4 is substituted in equation 3, and the high temperature limit for it is used to evaluate the appropriate traces. Consequently, the second moment for the pair can be written as

$$M_2(\alpha,\beta) = (3/4)\gamma^4\hbar^2 r_{\alpha\beta}^{-6}(1-3\cos^2\theta_{\alpha\beta})^2 \left[\frac{2\langle I(I+1)\rangle_\alpha\langle I(I+1)\rangle_\beta}{\langle I(I+1)\rangle_\alpha + \langle I(I+1)\rangle_\beta}\right] \qquad (5)$$

where γ is the gyromagnetic ratio of the proton, $\theta_{\alpha\beta}$ is the angle between $\vec{r}_{\alpha\beta}$ and the external magnetic field, and $\langle I(I+1)\rangle_\alpha$ is the value of $\langle I(I+1)\rangle_p$ for the molecule α. This result is extended to phase II of solid methane by considering all types of nearest-neighbor pairings.

For molecules on the two disordered sublattices in solid methane there are 12 nearest neighbors, each of which lies on an ordered sublattice. Similarly, each molecule on the six ordered sublattices has eight nearest neighbors also on ordered sublattices, as well as four nearest neighbors on disordered sublattices. Since the final result will be applied to polycrystalline lattices, a separate ensemble average is taken over space and spin factors in equation 5. Also, nearest-neighbor interactions dominate equation 5, so that the appropriate ensemble average for the spin factor can be considerably simplified by averaging only over the nearest neighbor pairs, hence

$$\overline{\langle I(I+1)\rangle_\alpha\langle I(I+1)\rangle_\beta} = (1/4)\{\langle I(I+1)\rangle_D\langle I(I+1)\rangle_D\} + (3/4)\{\langle I(I+1)\rangle_D[(2/3)\langle I(I+1)\rangle_O + (1/3)\langle I(I+1)\rangle_D]\} \qquad (6a),$$

and

$$\overline{\langle I(I+1)\rangle_\alpha + \langle I(I+1)\rangle_\beta} = (1/4)\{\langle I(I+1)\rangle_O + \langle I(I+1)\rangle_D\} + (3/4)\{\langle I(I+1)\rangle_O + [(2/3)\langle I(I+1)\rangle_O + (1/3)\langle I(I+1)\rangle_D]\} \qquad (6b),$$

where the subscripts O and D indicate average values of $\langle I(I+1)\rangle_p$ taken separately over ordered and disordered sublattices.

The spin factor averages in equations 6a and 6b can be further simplified by collecting like terms in $\langle I(I+1)\rangle_O$ and $\langle I(I+1)\rangle_D$. Finally, taking the powder average over $r_{\alpha\beta}$ and $\theta_{\alpha\beta}$ in eq FCC lattice gives the desired result for the second moment in

phase II of solid methane

$$M_2 = \frac{5.5225 \times 10^4}{d^6} \times \frac{[2\langle I(I+1)\rangle_0[\langle I(I+1)\rangle_0 + \langle I(I+1)\rangle_D]}{3\langle I(I+1)\rangle_0 + \langle I(I+1)\rangle_D} \quad (10^{-8}T^2) \qquad (7)$$

where d is the lattice constant in Å. The proton second moment is therefore sensitive to the temperature dependence of both the energy levels of the tunneling states (through $\langle I(I+1)\rangle_0$ and $\langle I(I+1)\rangle_D$), and the lattice parameter d. Highly accurate values of d for thermal equilibrium populations of the proton spin-symmetry species are known from the X-ray studies by Aadsen (2) and the thermal expansion measurements of Manzhelii et al. (20). A composite summary of their measured values of d is shown in Figure 4.

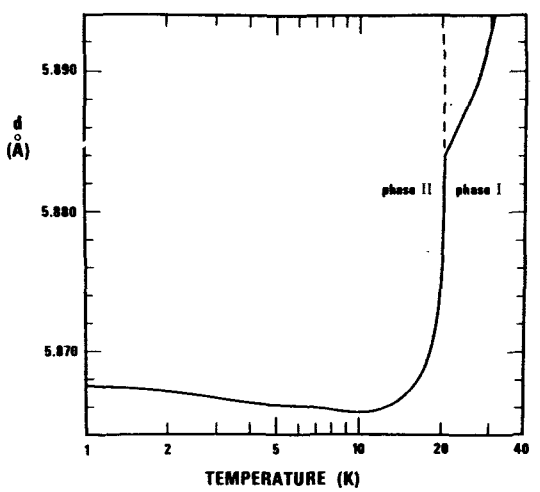

Figure 4. Temperature dependence of the FCC lattice parameter d in solid CH_4 from thermal expansion and X-ray diffraction experiments.

The temperature dependence of the lattice parameter is small enough that, even at the discontinuous phase transition at 20.4 K, it does not produce observable effects on the proton second moment at the present levels of accuracy (±5%). However, with pulsed, wideline, Fourier transform NMR spectroscopy (21), the second moment in solid methanes can be determined to an accuracy of ±0.5%. Fourier transform techniques should therefore make possible a future observation of the ~2% change in the proton second moment near 20.4 K associated with the change of d between phase I and phase II.

The most significant contribution to the variation of the proton second moment with temperature in equation 3 comes from the variation of $\langle I(I+1)\rangle_p$ on the respective sublattices. Equilibrium values of the proton second moment for "short-term" and "long-term" conversion have been calculated from equation 3 using the data of Figures 2 and 4. In Figure 5 the results are compared with the "equilibrium" experimental values of the second moment observed with a sample of solid CH_4 containing approximately 500 ppm O_2 impurities in the gas phase at room temperature. The existence of two distinct conversion rates is clearly seen by the consistency between the initial experimental value of the second moment measured at ~2.0 K and the "short-term" equilibrium curve calculated by forbidding conversion processes on the 6 ordered sublattices. The agreement between the observed values of the proton second moment and the values calculated from Nijman's theory is satisfactory. It should be noted that our values for the second moment at 8.5 K and 19 K may not have been determined under true equilibrium conditions. However, our experimental results for both the second moment and the mean square proton angular momentum per molecule in the vicinity of 20.4 K agree with a reduction in the mean A-T tunnel splitting on the disordered sites as observed by Press and Kollmar (15) when the temperature approached the phase I - phase II transition from below. The energy levels in this region are shown by dashed lines in Figure 2 because their width increases rapidly near the

transition temperature.

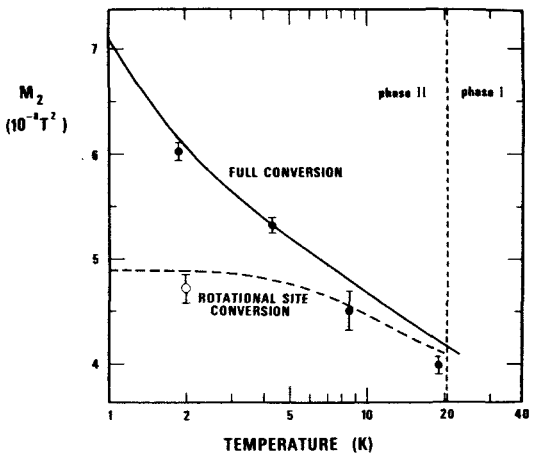

Figure 5. A comparison of observed and calculated values of the short and long term equilibrium proton second moments in solid methane as a function of temperature. The curves were obtained from equation 7. The solid methane contained trace oxygen impurities.

IV. Rates of Proton Spin Conversion

Proton spin conversion in pure solid CH_4 has been explained in terms of the physical mechanism that gives rise to such different conversion rates of the ordered and disordered sublattices in phase II (7). Observations of conversion by neutron scattering (22) and NMR (9) agree satisfactorily on the conversion rates, and indicate that spin-symmetry populations approach equilibrium exponentially with separate time constants of ~1/2 hour and ~150 hours respectively on the 2 disordered and 6 ordered sublattices at a temperature of ~1.8 K. The conversion rates in solid CH_4 and solid CH_3D (12) depend on the thermal history of the samples, and reliable rates can only be established in crystals whose orientational sublattice structure has been properly annealed.

The catalysis of proton spin conversion in methane by O_2 impurities is not yet well understood. A major difficulty appears to be the achievement of a uniform solid solution of oxygen in methane. Our experiments have shown that the conversion rate depends on the thermal history of sealed samples containing a fixed amount of oxygen. One sample containing 500 ppm O_2 displayed at 2 K an unusually long conversion time constant of 25 hours for molecules on the ordered sublattices (17). Another sample containing 960 ppm O_2 converted at 1.8 K in less than 1 hour (21), which is in better agreement with other experiments (23,24). This experience indicates that it is not possible by present techniques to control the uniformity of oxygen impurities in solid methane in order to make quantitative studies of the dependence of the proton spin conversion rate on concentration of oxygen impurities in the lattice. More uniform dispersions of paramagnetic impurities in solid methane can be obtained by γ-irradiation (25), and this approach has been very useful in the study of the properties of solid CH_4 below 1 K.

V. Conclusions

This review has shown how useful nuclear magnetic interactions can be as probes of the molecular dynamics of solid methane. In particular, it is fortunate that ^{13}C has a sufficiently large natural abundance and a strong enough magnetic moment to serve as a practical internal reference nucleus to monitor the absolute value of $\langle I(I+1)\rangle_p$. The long term stability of this internal "spin thermometer" provided the cornerstone for the NMR measurement of the proton spin-symmetry conversion rate on the ordered sublattices in phase II of solid methane below 4 Kelvin.

Retrospectively, it is surprising that a full generation of scientific effort was necessary to understand just the intensity and linewidth of the observed proton resonance in solid CH_4.

But now that more information is available about the ways this simple tetrahedral molecule forms orientational sublattices in the solid state, other questions can be raised. The nature of the "reorientational" processes that supress the intramolecular dipolar broadening at very low temperatures are not well understood at present. It would be desirable to study these by pulsed NMR techniques. Such experiments have not yet been done in sufficient detail below 4 Kelvin in pure CH_4 because of the very long equilibration times that are required.

It is much more convenient for experimentalists to observe NMR relaxation rates in the partially deuterated solid methanes, which promptly reach spin-species equilibrium. However, there are formidable challenges in extending the present theory of proton spin relaxation in solid methane (26) to the deuterated isotopes. Not only is the problem complicated by the reduced rotational symmetry of the deuterated molecules, but the sublattice structure in phase II and phase III of the partially deuterated solid methanes is not as well understood as it is in solid CH_4.

Future progress will undoubtedly come via pulsed NMR experiments on solid CH_4 and solid CH_3D at lower temperatures and higher pressures. There should be ample opportunity for yet another generation of physicists and chemists to make important discoveries about the properties of this family of simple molecular solids.

Acknowledgement

This research was supported in part by the Natural Sciences and Engineering Research Council of Canada.

REFERENCES

[1]J. Bonhoure and R. Pello, Metrologia 14, 175 (1978).

[2]D. R. Aadsen, Ph.D. Thesis, University of Illinois, Urbana (1975) [unpublished].

[3]H. M. James and T. A. Keenan, J. Chem. Phys. 31, 12 (1959).

[4]C. H. Anderson and N. F. Ramsey, Phys. Rev. 149, 14 (1966).

[5]A. W. Maue, Ann. der Physik (Leipzig) 30, 555 (1937).

[6]K. P. Wong, J. D. Noble, M. Bloom, and S. Alexander, J. Mag. Reson. 1, 55 (1969).

[7]A. J. Nijman and A. J. Berlinsky, Can. J. Phys. 58, 1049 (1980).

[8]R. F. Code and J. Higinbotham, Can. J. Phys. 54, 1248 (1976).

[9]J. Higinbotham, B. M. Wood, and R. F. Code, Phys. Lett. 66A, 237 (1978).

[10]R. F. Code, Rev. Sci. Instrum. 46, 661 (1975).

[11]J. Higinbotham, R. F. Code, and B. M. Wood, Phys. Rev. B14, 4773 (1976).

[12]J. Higinbotham, B. M. Wood, and R. F. Code, Can. J. Phys. 57, 1752 (1979).

[13]H. S. Sandhu, J. Lees, and M. Bloom, Can. J. Chem. 38, 493 (1960).

[14]J. Higinbotham and R. F. Code, Can. J. Phys. 60 1770 (1982).

[15]W. Press and A. Kollmar, Solid State Commun. 17, 405 (1975).

[16]A. Heidemann, W. Press, K. J. Lushington, and J. A. Morrison, J. Chem. Phys. 75, 4003 (1981).

[17]J. Higinbotham, Ph.D. Thesis, University of Toronto (1978) [unpublished].

[18]A. J. Nijman and N. J. Trappeniers, Physica (Utrecht) 95B, 147 (1978).

[19]A. J. Nijman, Ph.D. Thesis, University of Amsterdam (1977).

[20]V. G. Manzhelii, A. M. Tolkachev, A. N. Aleksandrovskii, V. B. Kolshenev, and V. I. Kuchnev, J. Physique, Colloque C6 (Supplement to Vol. 38), C6-1021 (1978).

[21]B. M. Wood, Ph.D. Thesis, University of Toronto (1982) [unpublished].

[22]K. J. Lushington and J. A. Morrison, Can. J. Phys. 55, 1580 (1977).

[23]K. J. Lushington, Ph.D. Thesis, McMaster University, Hamilton (1977) [unpublished].

[24]P. van Hecke and L. van Gerven, Physica (Utrecht) 68, 359 (1973).

[25]B. Bouchet and H. Glattli, J. Physique - Lettres 42, L159 (1981).

[26]M. Sprik, T. Heijmans and N. J. Trappeniers, Physica 112 B + C 285 (1982).